RESEARCH ARTICLE

Different protein metabolic strategies for growth during food-induced physiological plasticity in echinoid larvae

Aimee Ellison, Amara Pouv and Douglas A. Pace*

ABSTRACT

Food-induced morphological plasticity, a type of developmental plasticity, is a well-documented phenomenon in larvae of the echinoid echinoderm, *Dendraster excentricus*. A recent study in our lab has shown that this morphological plasticity is associated with significant physiological plasticity for growth. The goal of the current study was to measure several aspects of protein metabolism in larvae growing at different rates to understand the mechanistic basis for this physiological growth plasticity. Larvae of *D. excentricus* were fed rations of 1000 algal cells ml^{-1} (low-fed larvae) or 10,000 algal cells ml^{-1} (high-fed larvae). Relative protein growth rate was 6.0 and 12.2% day^{-1} for low- and high-fed larvae, respectively. The energetic cost of protein synthesis was similar for the two treatments at 4.91 J mg^{-1} protein synthesized. Larvae in both treatments used about 50% of their metabolic energy production to fuel protein synthesis. Mass-specific rates of protein synthesis were also similar. Large differences in mass-specific rates of protein degradation were observed. Low-fed larvae had relatively low rates of degradation early in development that increased with larval age, surpassing those of high-fed larvae at 20 days post-fertilization. Changes in protein depositional efficiency during development were similar to those of larval growth efficiency, indicating that differences in protein metabolism are largely responsible for whole-organism growth plasticity. Low-fed larvae also had alanine transport rates that were 2 times higher than those of high-fed larvae. In total, these results provide an explanation for the differences in growth efficiency between low- and high-fed larvae and allow for a more integrated understanding of developmental plasticity in echinoid larvae.

KEY WORDS: Developmental plasticity, Physiological plasticity, Protein metabolism, Larva, Physiology, Protein depositional efficiency, *Dendraster excentricus*

INTRODUCTION

The earliest stages of an organism's life are typically characterized by both rapid development and growth. The timing, rates and efficiencies of these processes can have important ramifications for the remainder of the organism's life. This is especially important for marine ectotherms, whose development and growth are sensitive to many different environmental parameters. Therefore, it is crucial to gain a foundational understanding of the molecular, biochemical, physiological and morphological pathways and strategies that are utilized during these unique moments where rates of growth and development are high, relative to later stages in life. Such an understanding is critical to predicting organismal responses in the face of rapid environmental changes, many of which are the result of anthropogenic activities.

An increase in biomass during early development, through the creation of new tissues as well as increases in biochemical reserves, occurs through accumulation of three primary biochemical substrates: proteins, lipids and carbohydrates. While there is interspecific variability in the importance of each, it is generally observed that proteins are the most important of these biomass constituents (Fraser and Rogers, 2007). Proteins comprise the majority of an organism's biomass and they serve as developmental and metabolic regulators because of their role as enzymes. Proteins are considered the most expensive molecules to synthesize (Hawkins, 1991; Houlihan, 1991; Berg et al., 2012), with each addition of an amino acid to a polypeptide chain costing, at a theoretical minimum, 4 ATP equivalents (Berg et al., 2012). Total costs of protein synthesis are likely much higher because of the additional costs of supporting processes such as amino acid transport, RNA synthesis and protein trafficking. Proteins also undergo relatively high rates of turnover in which they are degraded and resynthesized, adding another substantial energetic cost as a result of the ATP-dependent nature of ubiquitin targeting and proteasomal degradation (reviewed in Finley, 2009). These processes are collectively classified as protein metabolism. A critical question that emerges from studies of protein metabolism and growth is whether protein growth is achieved primarily through increased synthesis rates or by decreased degradation rates (Fraser and Rogers, 2007). Another important question is whether protein growth rates can be enhanced by manipulating the efficiency of protein metabolism. For example, increased rates of protein growth could theoretically be supported by increasing protein depositional efficiency and/or decreasing the energetic cost of protein synthesis.

Much research examining growth and development during early life stages has focused on planktotrophic (feeding) marine invertebrate larvae. This is especially true for the larvae of echinoid echinoderms, where there is a relative wealth of information concerning rates of morphological growth and development and their sensitivity to critical environmental parameters (e.g. McEdward, 1984; Hart and Strathmann, 1994; Bertram and Strathmann, 1998; Reitzel et al., 2004; Byrne et al., 2008; Pan et al., 2015; Rendleman and Pace, 2018). In addition, several studies have assessed the biochemical and metabolic importance of protein metabolism during echinoid development (Marsh et al., 2001; Pace and Manahan, 2006, 2007a; Pan et al., 2015, 2018). These studies have clearly demonstrated that regulation of protein metabolism is a significant feature in determining organismal rates of growth and as well as an important response mechanism to environmental changes.

Echinoid larvae exhibit food-induced phenotypic plasticity (e.g. Hart and Strathmann, 1994; Miner and Vonesh, 2004; Soars et al., 2009; Adams et al., 2011). From a morphological perspective, the pluteus larva responds to different levels of unicellular algal food by changing the length of its larval arms (ciliated projections that create a feeding current that allows for the capture and ingestion of algal food),

Department of Biological Sciences, California State University Long Beach, Long Beach, CA 90084, USA.

*Author for correspondence (douglas.pace@csulb.edu)

D.A.P., 0000-0002-1598-3295

List of abbreviations

AE	assimilation efficiency
DOM	dissolved organic material
dpf	days post-fertilization
FAA	free amino acid pool
GGE	gross growth efficiency
MBL	midline body length
NGE	net growth efficiency
PDE	protein depositional efficiency
PGE	protein growth efficiency
PO	post-oral arm
RGR	relative growth rate
TOR	target of rapamycin

such that larvae fed low levels of food grow longer arms to increase their feeding ability while those fed high levels of food grow shorter arms and allocate resources towards faster growth (Strathmann et al., 1992; Miner, 2011). This response allows larvae fed high levels of food to attain metamorphic competency sooner, thereby reducing their time in the plankton and its associated dangers (Rumrill, 1990). It has recently been demonstrated that in conjunction with this morphological plasticity there is also significant physiological plasticity (Rendleman et al., 2018). Larvae of the echinoid *Dendraster excentricus* fed low levels of food have relatively high assimilation efficiency (compared with that of larvae fed high levels of food) that complements their increased feeding ability. This high assimilation efficiency is accompanied by similarly high growth efficiencies, including protein growth efficiency (the growth of protein biomass relative to the amount of protein ingested). While these high efficiencies quickly diminish over development and are rapidly surpassed by those of larvae fed high levels of food, they are clearly beneficial and allow the morphological and physiological plasticity responses to operate in tandem to enable the larvae to make the most of their limited food environment. While there have been no direct measurements of protein metabolism with regards to this plasticity response, some studies have indirectly provided support for differences in protein metabolism by way of thyroxine signaling (Heyland and Hodin, 2004) and target of rapamycin (TOR) signaling (Carrier et al., 2015).

The goal of the current study was to directly quantify components of protein metabolism – protein growth, synthesis, degradation, depositional efficiency and energetic costs – in larvae of *D. excentricus* during food-induced plasticity. Our hypothesis was that because of the absolute requirement of macromolecular synthetic pathways for supporting biomass growth, the variation in larval growth efficiencies during food-induced plasticity is mechanistically linked to changes in one or more of these protein metabolism variables. We discovered that mass-specific rates of protein synthesis, as well as costs of protein synthesis, were similar in larvae fed low and high levels of food. The most significant difference was in protein depositional efficiency (the amount of synthesized protein retained as biomass), indicating that differential rates of protein degradation provide the mechanism by which different rates of protein growth were achieved between larvae on the two diets. Our results provide a physiological mechanism to explain the previously observed differences in protein growth efficiency (Rendleman et al., 2018) resulting from physiological plasticity.

MATERIALS AND METHODS
Sand dollar collection, spawning and larval culturing
Dendraster excentricus Eschscholtz 1831 adults were collected from Los Angeles Harbor in San Pedro, CA, USA (33.7088, −118.2806).

Animals were kept in large coolers during transport to the California State University, Long Beach (CSULB) Marine Laboratory. The collected sand dollars were kept in 200 l tanks of flowing seawater at about 16°C for no longer than 3 days before being used for experiments. Coelomic injections of 0.5 mol l^{-1} KCl were used to induce gamete release. Sperm were diluted (1:1000) and gently mixed with eggs in sterile-filtered seawater (0.2 μm pore) until achieving a sperm to egg ratio of ∼5:1. Fertilization envelopes were counted to confirm successful fertilization (>90%). All cultures were reared at 16±1°C (mean±s.d.) in the CSULB marine laboratory. For each culture, eggs and sperm from 3 females and 3 males were combined for fertilization. Embryos were reared at a density of 5 individuals ml^{-1} in 20 l food-grade vessels (Cambro, Huntington Beach, CA, USA). Cultures were gently mixed using a motor-driven plastic paddle (Buehler Products, Kinston, NC, USA) at 6 rpm. Experimental results (unless otherwise noted) were derived from 3 independent cultures that were initiated during July 2017 (culture 1), February 2018 (culture 2) and July 2018 (culture 3).

After reaching the feeding larval stage, animals were divided equally between two treatment groups: low- and high-fed larvae. Larvae were fed *Rhodomonas* sp., an algae commonly used to rear echinoid larvae because of its ability to support robust growth and development in a laboratory setting (e.g. Strathmann, 1971; Schiopu et al., 2006; Rendleman et al., 2018). Low- and high-fed rations corresponded to 1000 and 10,000 algal cells ml^{-1}, respectively. Previous research (Rendleman et al., 2018) has demonstrated that these culture conditions result in the expression of both morphological and physiological plasticity and thus are appropriate for our analysis. Algae were cultured in Erlenmeyer flasks with sponge stoppers and grown using f/2 media. Algal cultures were always harvested for larval feeding at the end of their logarithmic growth phase. To minimize the potential for microbial growth and other non-specific effects related to algal nutrient media, cultures were centrifuged (Beckman Coulter Avanti J-E: 1000 **g**, 12 min, 10°C) to remove media, and algae were resuspended in fresh seawater before counting and addition to larval cultures. Algal concentration was determined using a BD Accuri C6 (BD Biosciences, San Jose, CA, USA) flow cytometer following established methods (Cucci et al., 1989; Lizárraga et al., 2017; Rendleman et al., 2018). Algal cells were identified by chlorophyll autofluorescence stimulated by a blue laser (488 nm) and detected after passage through a 585/40 nm filter. Gating parameters and the accuracy of flow cytometer counts were established and checked using serial dilution assays of *Rhodomonas* sp. and comparison against hemocytometer counts. Algal concentrations in each larval culture were checked daily and restocked to the target feeding concentration to ensure consistent feeding conditions. High-fed larval cultures were terminated at 25 days post-fertilization (dpf) because a large proportion of larvae metamorphosed in the culture vessels. Low-fed larval cultures were studied until 42 dpf at which point there were not enough larvae to continue the analysis. Instantaneous mortality rates (m) of all cultures were determined using the equation $N_t = N_0 e^{-tm}$ (Rumrill, 1990), where N_0 is the number of larvae at 3 dpf, N_t is the number of larvae remaining at 23 dpf (a common range the two both feeding treatments was used), and t is the total time, 20 days.

Larval morphometrics
The occurrence of morphological plasticity was confirmed by linear measurements of low- and high-fed larvae. Because it has been demonstrated that the feeding conditions used here result in morphological plasticity, the current study only examined one of the cultures (culture 3) as a confirmation. Post-oral (PO) arm length

and mid-line body length (MBL) were measured as described in Rendleman et al. (2018). Measurements were made at 3, 5, 7, 10, 12, 15 and 20 dpf. Ten larvae from each treatment were removed and photographed using a QIClick digital camera mounted on an Olympus BX51 compound microscope. Lengths were then determined using ImageJ software calibrated using an image of a stage micrometer.

Protein biomass growth
Throughout larval development, triplicate samples of 500 larvae were taken for measuring protein biomass. Larval concentration was estimated using a Sedgewick Rafter counting chamber. Samples of known concentration were placed in 1.5 ml Eppendorf microcentrifuge tubes, spun at 1000 g (4°C) for 2 min and excess seawater removed by aspiration. Samples were then stored at −80°C until protein biomass was analyzed (within 4 weeks of sample being taken). Protein biomass was determined using a BCA Protein Assay Kit (Thermo Fisher Scientific). Previously frozen larval samples were removed from −80°C storage and resuspended in 500 µl of NANOpure water (Barnstead, Thermo Fisher Scientific) and sonicated (30% amplitude, 3 pulses at 2 s each while on ice). Three aliquots of each preparation (technical replicates) were run for protein content following the manufacturer's instructions. For all determinations of protein content, known absolute amounts of bovine serum albumin (BSA) were used to construct a standard curve for quantification of protein content from spectrophotometric absorption values (562 nm). Protein biomass values were used to quantify biomass growth rates as well as to standardize physiological rates to biomass (e.g. respiration, amino acid transport and protein synthesis rates). Relative growth rate (RGR, % protein mass day^{-1}) was calculated using the following equation (Conceição et al., 1998):

$$\text{RGR} = (e^g - 1) \times 100, \qquad (1)$$

where:

$$g = \frac{\ln \text{protein}_2 - \ln \text{protein}_1}{T_2 - T_1}, \qquad (2)$$

e is 2.718 (inverse of the natural log), T_1 and T_2 are the developmental time points where protein biomass samples were taken, and protein$_1$ and protein$_2$ are the protein biomass values (in ng individual^{-1}) for the respective time points. The RGR was calculated for every interval in which protein values were taken, resulting in 6 estimates per culture for low-fed larvae and 4–5 estimates per culture for high-fed larvae.

Ingestion rate
Daily algal ingestion rate was measured in all 3 cultures as described in Rendleman et al. (2018). Algal ingestion was determined by measuring the decrease in algal concentration ∼24 h after restocking each larval culture vessel to its target concentration. Algal concentration in vessels was determined using a BD Accuri™ C6 flow cytometer. Three algal samples (75 µl each) were removed from each culture vessel using a 50 µm-pore Nitex mesh to ensure no larvae entered the sample. The volume of sample necessary to count 100,000 cells was recorded. Variation between the 3 replicate algal samples for measuring ingestion rate was typically no larger than 10% (coefficient of variation). Three control vessels (3 l each, mixed with similarly proportioned paddles driven by small Beuhler motors) containing only algae were similarly measured and used to correct for any changes in algal concentration not attributed to larval feeding. Daily estimation also ensured that despite differences in feeding rate, low- and high-fed larvae were always restocked to their target algal

concentrations. The following equation was used to determine ingestion rate (IR; algal cells larva^{-1} day^{-1}):

$$\text{IR} = \frac{[((C_i - C_f)_{\text{Exp}} - (C_i - C_f)_{\text{Control}}) \times V]}{t \times n}. \qquad (3)$$

C_i and C_f represent the initial and final algal concentration (algal cells ml^{-1}), respectively, for the experimental (Exp; containing algae and larvae) and control (Control; containing only algae) vessels. The initial algal concentration was never assumed but always measured after restocking to the target concentration for each feeding treatment, thereby controlling for possible variation resulting from estimation of total culture volume, which was accomplished using the volumetric markings on the culture vessels. V is the volume of the culture vessels (in ml), t is the duration between the initial and final algal concentration measurements (typically between 20 and 24 h) and n is the number of larvae in the experimental vessel for which ingestion rates were estimated. The concentration of larvae in the vessels was determined 3 times per week (during water changes using a Sedgewick Rafter counting chamber) and used with culture volume to estimate larval numbers. For IR determinations on a non-water change day, larval number was estimated by interpolating from larval estimates preceding and succeeding that measurement. These IR values were then used to directly determine the amount of energy ingested through algal feeding and subsequently used to support measured physiological rates (e.g. growth, respiration, protein synthesis). Because there were instances when larvae ate most of the food provided within the 24 h interval (especially later in development), these estimates are not reflective of their feeding capacity.

Respiration rate
Larval respiration rate was determined in all 3 cultures as described in Rendleman et al. (2018), using the µBOD method (Marsh and Manahan, 1999). Sterile filtered oxygen-saturated seawater was placed in 11 custom-made µBOD vials (∼800 µl volume) and larvae (50–600 individuals, depending on developmental stage) were micro-pipetted into eight µBOD vials. The additional three vials contained only filtered seawater and served as blanks to account for non-larval consumption of O$_2$ (e.g. microbial respiration). The vials were then incubated at 16°C for 3 h, after which time the oxygen content was measured using a polarographic oxygen sensor (Strathkelvin Instruments). Vials were centrifuged (50 g) and approximately 400 µl of seawater was removed with a gas-tight syringe and injected into the oxygen sensor chamber (∼70 µl volume). After 1 min, the time and oxygen concentration were recorded. The number of larvae in each vial was counted for each treatment and oxygen consumption (pmol O$_2$ h^{-1}) was linearly regressed against the number of individuals in each vial to determine pmol O$_2$ h^{-1} individual^{-1}. For all respiration rates recorded, no evidence of concentration-dependent artifacts was observed (i.e. total O$_2$ consumed increased linearly with increasing number of larvae in each µBOD vial).

Efficiency analyses
Data for daily ingestion rate, protein growth rate and respiration rate were used to construct energetic efficiency models for assimilation efficiency (AE), gross growth efficiency (GGE), net growth efficiency (NGE) and protein growth efficiency (PGE). These values were determined following the protocols of Rendleman et al. (2018). The following equations were used for the respective

efficiencies:

$$AE = [(M + G)/I] \times 100, \qquad (4)$$

$$GGE = [G/I] \times 100, \qquad (5)$$

$$NGE = [G/(G + M)] \times 100, \qquad (6)$$

$$PGE = (\text{protein growth/protein ingested}) \times 100. \qquad (7)$$

M is the energy metabolized and measured through oxygen respiration rates. Oxygen consumption values were converted to energetic units using the oxyenthalpic value of 484 kJ mol^{-1} O$_2$ (Gnaiger, 1983). G is biomass growth and was determined using changes in protein biomass. Protein values were converted to energetic equivalents using a conversion of 24 kJ g^{-1} (Gnaiger, 1983; Schmidt-Nielsen, 1997). I represents energy acquired through ingestion. Ingestion rates of algal cells were converted to energetic units using the specific energetic content of *Rhodomonas* sp.: 2.25 μJ algal cell^{-1} (Vedel and Rissgård, 1993). Protein ingested was determined using the protein content of *Rhodomonas* sp.: 0.053 ng protein algal cell^{-1} (Rendleman et al., 2018). In order to accurately model these efficiency metrics over development, primary data (ingestion, protein growth, respiration and protein synthesis) from all three cultures were used to create a best-fit model describing how each variable changed throughout larval development in low- and high-fed larvae. For each culture, the linear regression values (slope and y-intercept) were determined for the log$_{10}(x)$ transformed data (ingestion, respiration or protein biomass) plotted against dpf. In order to take into account the slight variation in sample size per culture (i.e. the number of developmental time points measured), the weighted mean for each regression value was calculated (Sokal et al., 1987). These weighted average regression values were used to model changes in each respective variable throughout larval development for low- and high-fed larvae.

Rate of protein synthesis

The rate of protein synthesis was determined as described in other studies of echinoderm larvae (Pace and Manahan, 2006; Pace et al., 2010; Pan et al., 2015). ^{14}C-Alanine (Perkin Elmer), was used as a tracer to follow the rate of incorporation of amino acids into protein. Previous studies on echinoid larvae have shown alanine to be optimal for use as a radiolabeled tracer as it is transported rapidly from seawater into the free amino acid (FAA) pool and subsequently incorporated into the protein pool in sufficient amounts to be accurately measured by HPLC and liquid scintillation counting (Marsh et al., 2001; Pace and Manahan, 2006, 2007a). As part of this measurement, rates of alanine transport were also determined (described below). Each protein synthesis determination was a 3-part kinetic assay determining (1) the rate of total alanine incorporation into larvae (i.e. alanine transport rate), (2) the change in specific activity of alanine in the precursor FAA pool and (3) the rate of alanine incorporation into larval protein. The three kinetic assays were run in parallel from the same stock of larvae exposed to the ^{14}C-alanine tracer. For each experiment, a known number of larvae was exposed to 10–20 μmol l^{-1} ^{14}C-alanine in 10 ml of seawater (total radioactivity 5 μCi). Each assay was composed of 6 individual time points, taken over the course of 20–25 min, used for calculating linear rates of change for each respective variable. The short time frame minimizes the effect of protein degradation, where ^{14}C-alanine re-enters the FAA pool as a result of protein degradation. The samples of larvae were placed onto an 8 μm filter (Nucleopore) and washed 3 times with fresh seawater to remove unincorporated radioactivity. Using these data,

whole-animal rates of protein synthesis were determined using the following equation:

$$PS = \frac{d}{dt}\left(\frac{S_p}{S_{FAA}}\right) \times \frac{MW_p}{S_m}, \qquad (8)$$

where PS is the protein synthesis rate (ng larva^{-1} h^{-1}), S_p is the radioactivity in the total protein pool (procedure described below), S_{FAA} is the specific activity of the FAA pool (procedure described below), MW$_p$ is the average molecular weight of an amino acid in *D. excentricus* and S_m is the mole per cent (mol %) of the amino acid used in protein. The following descriptions detail the methods for acquiring the different datasets represented in Eqn 8.

Specific activity of the FAA pool (S_{FAA})

S_{FAA} was determined through HPLC separation of the FAA pool and liquid scintillation counting (Beckman Coulter LS 6500) of the alanine elution peak. A known number of larvae were exposed to 10–20 μmol l^{-1} ^{14}C-alanine in 10 ml of seawater (total radioactivity 5 μCi). Six 500 μl samples were taken regularly over a 25 min interval to quantify the temporal increase in S_{FAA}. The FAA for each sample was extracted in 70% ethanol and alanine was separated from other amino acids using reverse phase HPLC (Lindroth and Mopper, 1979). Amino acids were detected using precolumn derivatization with ortho-phthalaldehyde (OPA; Sigma Aldrich P0657). A dual gradient solvent system in conjunction with a C-18 reverse phase column separated amino acids based on hydrophobicity. The gradient system progressed from hydrophilic (Solvent A: 80% 50 mmol l^{-1} sodium acetate, 20% methanol) to hydrophobic (Solvent B: 20% 50 mmol l^{-1} sodium acetate, 80% methanol). Alanine was quantified through peak area comparison with standards of known concentrations. The alanine elution peak was collected in a fraction collector and its radioactivity was determined by liquid scintillation counting. This method allowed for accurate determination of changes in the precursor specific activity in dpm pmol^{-1} alanine. This value was then used to correct for the radioactive incorporation rate of ^{14}C-alanine into the protein pool.

Radioactivity in the total protein pool (S_p)

Larvae sampled for determining the rate of ^{14}C-alanine incorporation into protein were immediately frozen in liquid nitrogen. For each sample, 500 larvae were collected. These samples were subsequently sonicated and total protein was precipitated using cold 5% trichloroacetic acid (TCA). The protein precipitate was collected on a GF/C glass microfiber filter (Whatman, Sigma Aldrich) and then mixed with EcoScint (Fisher Scientific) scintillation cocktail. Radioactivity of the protein was determined using a Beckman Coulter LS 6500 liquid scintillation counter. The amount of ^{14}C-alanine incorporated into total protein was converted to total alanine incorporation using the measured intracellular specific activity (^{14}C per mol total alanine in the FAA pool, aka S_{FAA}). By standardizing S_p by S_{FAA} over the duration of the experiment, the rate of total alanine incorporation was determined (pmol alanine larva^{-1} h^{-1}).

Average molecular weight of an amino acid in *D. excentricus* and mol % alanine in total protein (MW$_p$ and S_m)

In order to convert alanine incorporation rate into total amino acid incorporation rate (i.e. rate of protein synthesis), the amino acid composition of larval protein (i.e. mol % composition of protein; S_m) and the average molecular weight of an amino acid in the protein pool (MW$_p$) were determined. Amino acid composition

was determined by UC Davis Core Facility using an amino acid analyzer. Protein was extracted in 5% TCA and then acid-hydrolyzed in 6 mol l^{-1} HCl with 0.5% phenol at 110°C for 24 h under vacuum. The acid-hydrolyzed protein was then run on a cation exchange chromatographer. Post-column ninhydrin derivitization was used to obtain amino acid composition.

Total alanine larval transport

Alanine transport rate was determined by measuring the increase in total larval radioactivity. While transport rate is not part of the protein synthesis calculation, this was conducted in conjunction with protein synthesis experiments. These data also allowed us to construct radioactivity budgets to ensure the sum of ^{14}C-alanine incorporation into the FAA and total protein pool was equal to the total radioactive incorporation measured as alanine transport. Larvae were sampled and placed in a liquid scintillation vial with 5 ml of EcoScint cocktail (Fisher Scientific). Samples were counted in a Beckman Coulter LS 6500 scintillation counter. ^{12}C-Alanine (i.e. 'cold' alanine) was added to the experimental vial to bring the final concentration to 20 µmol l^{-1}. Alanine transport rate was then corrected using the necessary ^{14}C:^{12}C-alanine ratio (hot:cold ratio). Alanine transport rate was also determined in experiments using the protein synthesis inhibitor anisomycin, in order to assess whether the inhibitor had any non-specific effects.

Cost of protein synthesis

The energetic cost of protein synthesis (J mg^{-1} protein synthesized) was calculated using two different approaches. Both approaches utilized respiration rate and protein synthesis rate data, acquired as described above. A direct approach used inhibition of protein synthesis to calculate its cost at specific developmental time points (i.e. before feeding larvae as well as in low- and high-fed larvae at 11 and 19 dpf). This approach measured the change in respiration and protein synthesis when in the presence or absence of the eukaryotic protein synthesis inhibitor anisomycin (Sigma-Aldrich), which has been shown to be highly effective and specific (Fenteany et al., 1995; Pace and Manahan, 2007a). Anisomycin was used at a concentration of 20 µmol l^{-1}. For calculating the cost of protein synthesis, the rate of oxygen consumption was converted to energetic units using an oxyenthalpic conversion of 484 kJ mol^{-1} O$_2$ (Gnaiger, 1983). Cost was determined by dividing the difference in metabolic rate by the difference in protein synthesis rate when in the presence of the inhibitor. Therefore, the efficacy of the inhibitor was never assumed but was empirically determined. Additionally, the rate of alanine transport was measured during inhibitor exposure as a check for potential non-specific effects of the inhibitor.

We also used an indirect, correlative approach to determine the cost of protein synthesis throughout larval development. Here, the relationship between changes in respiration rate and protein synthesis rate over development was assessed. These values represent normal physiological rates (i.e. no inhibitors were employed). Respiration rate was plotted (ordinate) against protein synthesis rate (abscissa) and tested for a significant relationship. The slope of this relationship therefore represents the cost of protein synthesis (the change in energy consumption rate per unit increase in protein synthesis rate).

Protein depositional efficiency and rate and cost of protein degradation

In order to assess the efficiency of protein metabolism of low- and high-fed larvae, protein depositional efficiency (PDE) was determined by standardizing the amount of protein growth to the total amount of protein synthesized. PDE was calculated using the modeled data of protein growth and protein synthesis using the following equation:

$$PDE = (\text{protein growth/protein synthesized}) \times 100. \quad (9)$$

An alternative PDE analysis was also conducted in order to understand how PDE changes during development while controlling for differences in rates of growth between low- and high-fed larvae. Here, PDE was determined for specific amounts of total protein growth. In this assessment, PDE and the corresponding rates of synthesis and degradation were determined after ∼55 ng of protein growth (representing early development) and ∼650 ng of protein growth (representing late development).

The rates of protein degradation were calculated as the difference between the modeled rates of protein synthesis and protein growth. The cost of protein degradation was taken from Pan et al. (2018) as 0.14 kJ g^{-1} protein degraded. As specified in Pan et al. (2018), this cost is based on the primary analysis by Peth et al. (2013), where degradation is by the 26S proteasomal pathway. This estimate is based on the assumption that degradation occurs via the 26S pathway and requires 0.003 mol ATP g^{-1} protein, and that 45 kJ of energy are liberated with the hydrolysis of a mole of ATP (details in Pan et al., 2018).

Statistical analysis

Variation in morphological and physiological variables as a function of developmental time (dpf) and feeding treatment (low versus high) was evaluated with general linear models (GLMs). Replicate cultures were treated as a random factor so that within-treatment variation among cultures could be assessed. In the absence of a statistically significant interaction between main effects, analysis of covariance (ANCOVA) was used to compare adjusted mean values of the different feeding treatments; when there was a significant interaction, no further analysis was done. Prior to analyses, physiological variables were transformed using a $\log_{10}(x)$ function to correct for non-linearity, non-normality and unequal variances as necessary. Visual inspection of model residuals was done for every analysis.

Regression slopes and intercepts for the three independent cultures were pooled within feeding treatments as weighted mean averages and weighted mean standard deviations to parameterize models of rate changes during development (after Sokal et al., 1987). In cases where there was a significant block effect (indicative of culture to culture variation), data were still averaged because the main effects were always much larger than the block effect (as determined by eta squared, η^2, the ratio of effect sum of squares to total sum of squares; Thompson, 2006) and the general outcome remained the same. All analyses were performed using Minitab 18.

RESULTS

Development and induction of morphological plasticity

Both feeding treatments were effective in supporting larval growth and development (Fig. 1A). Average rates of mortality for the three cultures were similar between feeding treatments (ANOVA, $F_{1,5}$=7.71, P=0.57) at 0.067±0.023 and 0.056±0.023 day^{-1} (mean± s.d., n=3) for low- and high-fed larvae, respectively. Both low- and high-fed larvae were at the 4-arm pluteus stage at 3 dpf. The first observation of the 6-arm pluteus stage was at 10 and 6 dpf for low- and high-fed larvae, respectively. The first observation of larvae at the 8-arm pluteus stage was at 26 and 10 dpf for low- and high-fed larvae, respectively. High-fed larvae reached metamorphic
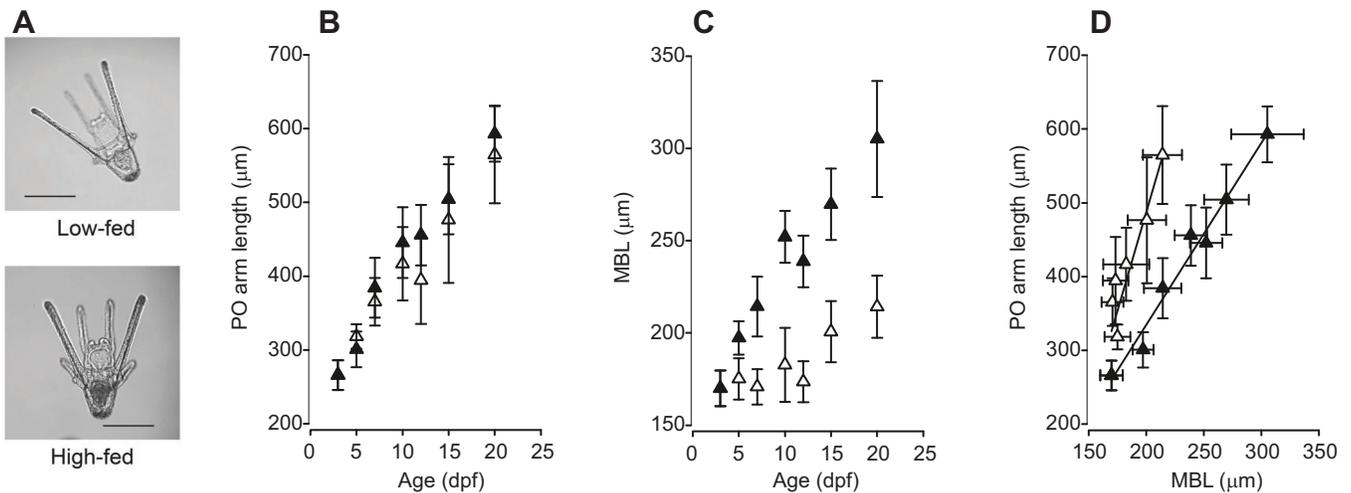
Fig. 1. Changes in larval morphology and expression of morphological plasticity in *Dendraster excentricus* larvae reared at low and high food concentrations. (A) Images of larvae fed 1000 algal cells ml^{-1} (low-fed larvae) or 10,000 algal cells ml^{-1} (high-fed larvae) at 7 days post-fertilization (dpf). Scale bars: 200 μm. (B) Post-oral (PO) arm growth in low- and high-fed larvae. There was no significant treatment effect (ANOVA, $F_{1,13}$=0.04, P=0.85) or interaction with larval age (ANOVA, $F_{1,13}$=1.44, P=0.26), indicative that PO arm length growth was similar in low- and high-fed larvae. (C) Midline body length (MBL) growth in low- and high-fed larvae. (D) PO arm growth as a function of MBL. The solid line represents the linear regression model for each feeding treatment. Low-fed: y=5.34x−581.0, r^2=0.84; high-fed: y=2.47x−159.3, r^2=0.98. There was a significant feeding treatment effect (ANOVA, $F_{1,13}$=11.36, P=0.007), indicative of low-fed larvae having a longer PO arm length for any given midline body length. Data in B–D are means±s.d.; white symbols indicate low-fed larvae and black symbols represent high-fed larvae. Data for morphology were from culture 3.

competency by 24 dpf, where it was observed that they were metamorphosing in the culture vessels. Low-fed larvae were not observed to reach metamorphosis in any of the culture vessels.

Despite the order of magnitude difference in available food, PO arm growth was similar between low- and high-fed larvae (ANOVA, $F_{1,13}$=0.04, P=0.85) (Fig. 1A,B) and there was no interaction between feeding treatment and larval age (ANOVA, $F_{1,13}$=1.44, P=0.26). In contrast, for MBL a significant interaction between feeding treatment and age was observed (ANOVA, $F_{1,13}$=27.76, P<0.001), indicative of faster rates of MBL growth in high-fed larvae (Fig. 1C). The relationship between PO length and MBL exhibited a significant feeding treatment effect (ANOVA, $F_{1,13}$=11.36, P=0.007), indicating that at any given MBL, low-fed larvae had a longer PO length (Fig. 1D). These results are similar to those in our previous study (Rendleman et al., 2018).

Physiological plasticity

Rates of protein growth (Fig. 2A), algal ingestion (Fig. 2B) and respiration (Fig. 2C) were measured to ensure the patterns of physiological plasticity that were documented in Rendleman et al. (2018) were observed in this study as well, which used identical culturing and treatment conditions. Larval protein biomass increased throughout development for both feeding treatments (Fig. 2A). There was a strong interaction between feeding treatment and larval age (dpf) (ANOVA, $F_{1,38}$=20.35; P<0.001; Table 1), indicative of protein biomass starting from a common value and high-fed larvae growing at a faster rate than low-fed larvae. By 23 dpf, low-fed larvae had a protein biomass of 309 ng larva^{-1}, while the value for high-fed larvae was 1420 ng larva^{-1} (using the common regression lines illustrated in Fig. 2A). At 42 dpf, low-fed larvae had a protein biomass of 763 ng protein larva^{-1}. RGR was significantly different in low- and high-fed larvae (ANOVA, $F_{1,5}$=13.8, P<0.05). RGR of high-fed larvae was 2 times faster (Fig. 2A, inset), at 12.2±1.6% day^{-1} versus 6.0±0.59% day^{-1} (means±s.e.m., n=3) for low-fed larvae. The rate of algal ingestion (Fig. 2B) increased with development for low- and high-fed larvae.

Ingestion rate was always higher in high-fed larvae and no statistical interaction was observed between feeding treatment and larval age (Table 1). Differences in feeding rate were reflective of the 10-fold difference in available algae. For example, at 25 dpf, rates of ingestion were 691 and 5230 algal cells day^{-1} individual^{-1} for low- and high-fed larvae, respectively. There was significant within-treatment variation for ingestion rate (e.g. dotted line in Fig. 2B for low-fed culture 1); however, the main effect of feeding treatment was much larger (Table 1). Larval rate of respiration (Fig. 2C) increased significantly with larval age ($F_{1,32}$=204, P<0.001; Table 1). There was a significant interaction between feeding treatment and larval age ($F_{1,32}$=9.51, P=0.004; Table 1), indicating that the rate of respiration increased faster in high-fed relative to low-fed larvae during development. There was significant within-treatment variation for respiration rate (e.g. dotted line in Fig. 2C for low-fed culture 1), but the main effect of feeding treatment was much larger (Table 1).

Rates of protein growth, algal ingestion and respiration were used to model physiological efficiencies relating to digestion and growth. The regression variables to model these changes in energy acquisition were determined by taking the weighted average regression variables for each metric (taking into consideration unequal sample sizes for each independent culture). These values and their standard deviations are given in Fig. S1. Using these values, the daily changes in energy acquired, respired and invested into growth were determined for low- and high-fed larvae (Fig. S2). These values were then used to construct the models for daily changes in AE, GGE, NGE and PGE (see Materials and Methods for details of calculations) and are displayed in Fig. 2D. For all efficiencies that were standardized to the amount of energy acquired (i.e. AE, GGE and PGE), a common pattern was observed. Low-fed larvae initially had high efficiencies that decreased rapidly as development proceeded. High-fed larvae had low efficiencies that increased rapidly during development. This resulted in high-fed larvae efficiencies surpassing low-fed efficiencies by 18 dpf. A comparison of these efficiencies at 24 dpf (the end of the high-fed
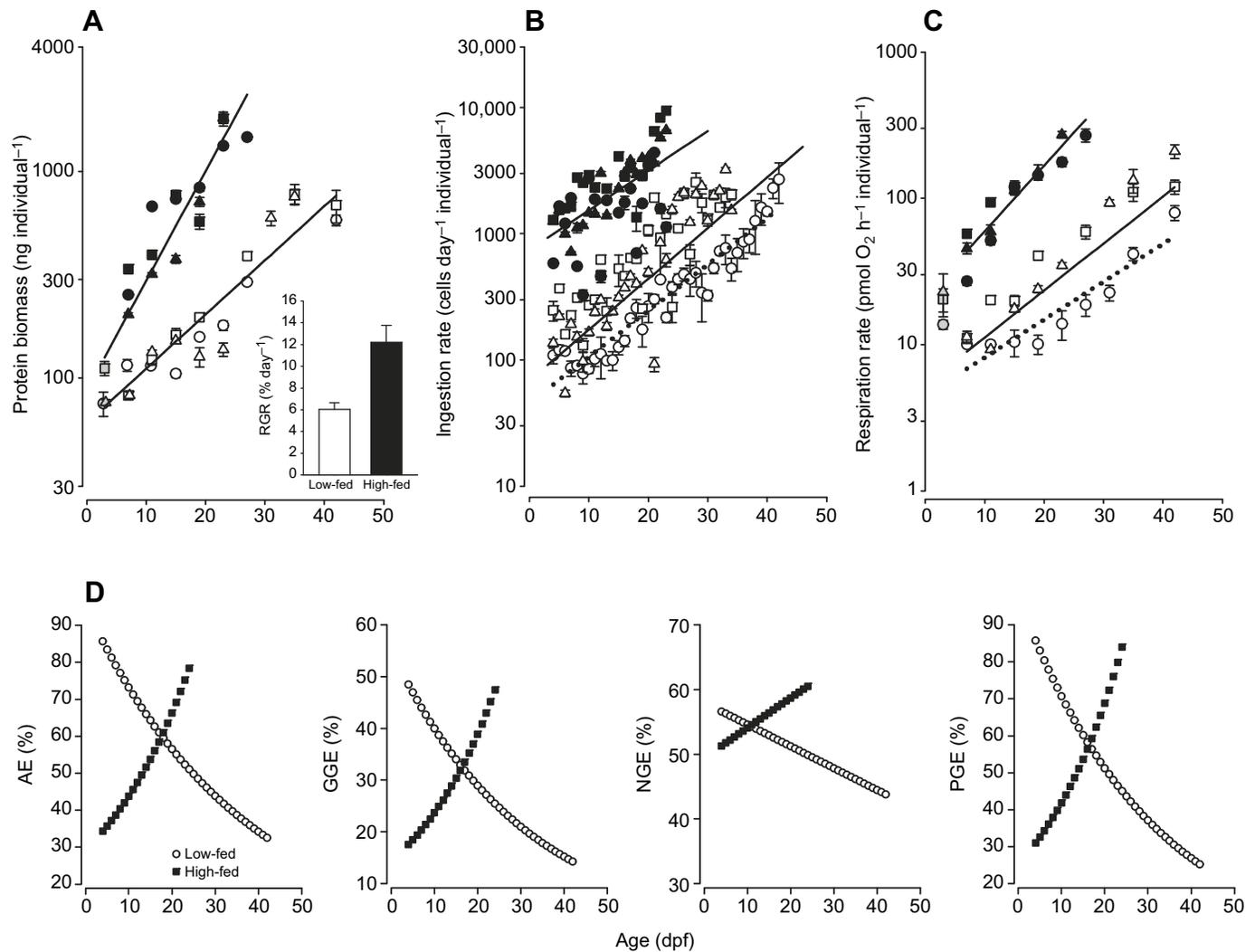
Fig. 2. Physiological parameters and energetic efficiencies of digestion and growth in low- and high-fed larvae of *D. excentricus*. (A) Changes in protein biomass (plotted on a log_{10} scale) before feeding (gray symbols) and in low-fed (white symbols) and high-fed (black symbols) larvae as a function of age. Data are means±s.e.m. (*n*=3). Regression lines show the pooled response for low- and high-fed larvae for all three cultures analyzed (culture 1, circles; culture 2, squares; culture 3, triangles). Inset: relative growth rate (RGR) for each treatment (means±s.e.m., *n*=3). (B) Ingestion rate (plotted on a log_{10} scale) in low-fed (white symbols) and high-fed (black symbols) larvae as a function of age. Data are means±s.e.m. (*n*=3). Regression lines are for all three cultures pooled for each feeding treatment. The dotted line represents independent regression of ingestion rate and larval age for low-fed larvae from culture 1 (white circles). (C) Respiration rate (plotted on a log_{10} scale) before feeding (gray symbols) and in low-fed (white symbols) and high-fed (black symbols) larvae. Data are means±s.e.m. (*n*=7). Regression lines are for all three cultures pooled for each feeding treatment (low- and high-fed). The dotted line represents independent regression of respiration rate and larval age for low-fed larvae from culture 1 (white circles). (D) Modeled daily efficiency measurements relating to digestion and growth in low- and high-fed larvae: AE, assimilation efficiency; GGE, gross growth efficiency; NGE, net growth efficiency; and PGE, protein growth efficiency. All values were determined using parameters from regression lines in A–C. See Figs S1 and S2 for information relating to regression values used for energetic modeling.

culture) shows that high-fed larvae had 1.6 times higher AE, and 2.0 times higher GGE and PGE than low-fed larvae. NGE also exhibited the same diverging pattern; however, low- and high-fed larvae started at a similar value of ∼53%, which increased to 61% in high-fed larvae and decreased to 49% in low-fed larvae by 24 dpf. After 24 dpf, values for low-fed larvae continued to decrease for all efficiency metrics with the following values at 42 dpf (the last day of monitoring for low-fed larvae): AE=32%, GGE=14%, NGE=44%, PGE=25%. Efficiency data were also standardized to the time of first observation of the 4-, 6- and 8-arm pluteus stages (Fig. S3A–D). AE, GGE and PGE were higher in low-fed than in high-fed larvae during early larval development (4- and 6-arm stage). However, by the 8-arm stage, these efficiencies were similar in low- and high-fed larvae. NGE (Fig. S3C) values were relatively similar at all three developmental stages.

Protein metabolism
Alanine transport rate
The rate of alanine transport increased with development for both low- and high-fed larvae (Fig. 3A), but the increase was faster in high-fed larvae as evidenced by a significant interaction between feeding treatment and larval age (ANOVA, $F_{1,32}$=21.55, *P*<0.001; Table 1). There was significant within-treatment variation for transport rate (e.g. dotted line in Fig. 3A for low-fed culture 1). When alanine transport rate was standardized to protein biomass (Fig. 3B), the developmental increase in rate was only marginally significant (ANOVA, $F_{1,32}$=3.92, *P*=0.06; Table 1). Mass-specific transport rate in low-fed was significantly higher than in high-fed larvae (ANOVA, $F_{1,32}$=4.49, *P*=0.042; Table 1). Adjusted mean mass-specific transport rate (inset, Fig. 3B) was ∼2 times higher for low-fed larvae than for high-fed larvae (i.e. 0.088 and 0.043 pmol h^{-1} μg^{-1} protein, respectively).

Table 1. Statistical analyses for physiological variables in *Dendraster excentricus* larvae reared at low and high food concentrations

Trait	Source	d.f.	MS	F	P
Protein biomass (ng protein individual^{-1}) (Fig. 2A)	Culture	2	0.021	0.93	0.40
	Treatment (low- and high-fed)	1	0.093	4.04	0.052
	dpf	1	5.38	238.87	<0.001
	Interaction (treatment×dpf)	1	0.11	20.35	<0.001
	Error	38	0.023		
Ingestion rate (algal cells day^{-1} individual^{-1}) (Fig. 2B)	Culture	2	2.35	52.86	<0.001
	Treatment (low- and high-fed)	1	6.14	138.19	<0.001
	dpf	1	8.23	185.31	<0.001
	Interaction (treatment×dpf)	1	0.095	2.14	0.146
	Error	151	0.044		
Respiration rate (pmol O$_2$ h^{-1} individual^{-1}) (Fig. 2C)	Culture	2	0.34	23.41	<0.001
	Treatment (low- and high-fed)	1	0.42	28.59	<0.001
	dpf	1	2.99	203.55	<0.001
	Interaction (treatment×dpf)	1	0.14	9.51	0.004
	Error	32	0.015		
Transport rate (pmol h^{-1} individual^{-1}) (Fig. 3A)	Culture	2	381.23	14.75	<0.001
	Treatment (low- and high-fed)	1	1.76	0.07	0.796
	dpf	1	3.37×10^3	130.39	<0.001
	Interaction (treatment×dpf)	1	557	21.55	<0.001
	Error	32	25.84		
Transport rate (pmol h^{-1} µg^{-1} protein) (Fig. 3B)	Culture	2	1.7×10^{-3}	2.83	0.074
	Treatment (low- and high-fed)	1	2.7×10^{-3}	4.49	0.042
	dpf	1	2.3×10^{-3}	3.92	0.056
	Interaction (treatment×dpf)	1	5.0×10^{-6}	0.01	0.931
	Error	32	6.0×10^{-4}		
Protein synthesis rate (ng protein h^{-1} individual^{-1}) (Fig. 4A)	Culture	2	0.047	0.94	0.401
	Treatment (low- and high-fed)	1	0.63	12.61	0.001
	dpf	1	3.83	76.87	<0.001
	Interaction (treatment×dpf)	1	0.055	1.10	0.302
	Error	32	0.050		
Protein synthesis rate (ng protein synthesized ng^{-1} protein biomass) (Fig. 4B)	Culture	2	0.068	0.90	0.417
	Treatment (low- and high-fed)	1	0.12	1.59	0.218
	dpf	1	0.44	5.79	0.022
	Interaction (treatment×dpf)	1	8.0×10^{-3}	0.11	0.747
	Error	32	0.075		
Correlative cost of protein synthesis (J mg^{-1} protein synthesized ng^{-1}) (Fig. 5B)	Culture	2	266	1.29	0.289
	Treatment (low- and high-fed)	1	1.09×10^3	5.29	0.028
	Protein synthesized	1	2.48×10^4	120	<0.001
	Interaction (treatment×dpf)	1	445	2.16	0.152
	Error	32	206		

Cultures were treated as a random blocking factor.

Protein synthesis rate

Amino acid composition (both S_m and MW_p) was similar for before feeding (3 dpf) and in low- and high-fed larvae (19 dpf) (Table S1). The mean (±s.d., $n=3$) percentage of alanine in total protein was 9.5±0.61%. The mean (±s.d., $n=3$) molecular weight of an amino acid in the total protein pool (MW_p) was 126.0±0.25 g mol^{-1}.

The rate of protein synthesis before feeding (3 dpf) was ~1 ng h^{-1} individual^{-1} (Fig. 4A). Upon initiation of feeding, both low- and high-fed larvae exhibited significant increases in the rate of protein synthesis (ANOVA, $F_{1,32}=76.87$, $P<0.001$; Table 1). As no significant interaction was observed between feeding treatment and larval age, rates increased similarly (Table 1). However, for any given age, high-fed larvae had a significantly higher protein synthesis rate than low-fed larvae (ANOVA, $F_{1,32}=12.61$, $P=0.001$; Table 1). Mass-specific rate of synthesis (i.e. fractional rate) ranged from 0.5 to 1.5% h^{-1} (Fig. 4B). Unlike whole-organism rates of protein synthesis, fractional rates of protein synthesis were similar between low- and high-fed larvae (ANOVA, $F_{1,32}=1.59$, $P=0.218$; Table 1), indicating that increases in whole-larval protein synthesis rate were driven by increases in protein biomass.

Rate and metabolic importance of protein degradation

Fractional rates of protein degradation (Fig. 4C) were modeled using the data for protein growth (Fig. 2A) and protein synthesis (Fig. 4A). This assumes that for growing organisms, the amount of protein degradation is equal to the difference between protein synthesized and protein grown (Hawkins, 1991; Houlihan, 1991). Unlike fractional rate of protein synthesis, there was a noticeable influence of feeding treatment on the rate of protein degradation. Fractional rates of protein degradation for low-fed larvae increased 17-fold (0.048 to 0.80 ng degraded ng^{-1} protein biomass) from 4 to 42 dpf. For high-fed larvae, rates decreased moderately from 0.37 to 0.25 ng degraded ng^{-1} protein biomass from 4 to 24 dpf. The percentage metabolism used to fuel these rates of degradation (Fig. 4C, inset) was low for both treatments, but increased for low-fed larvae from 0.1% to 1.8% of metabolism. High-fed larvae used about 0.5% of metabolism to fuel protein degradation.

### Energetic cost of protein synthesis

The energetic cost of protein synthesis at specific developmental time points (using the protein synthesis inhibitor anisomycin) was similar for before feeding and in low- and high-fed larvae (Fig. 5A)
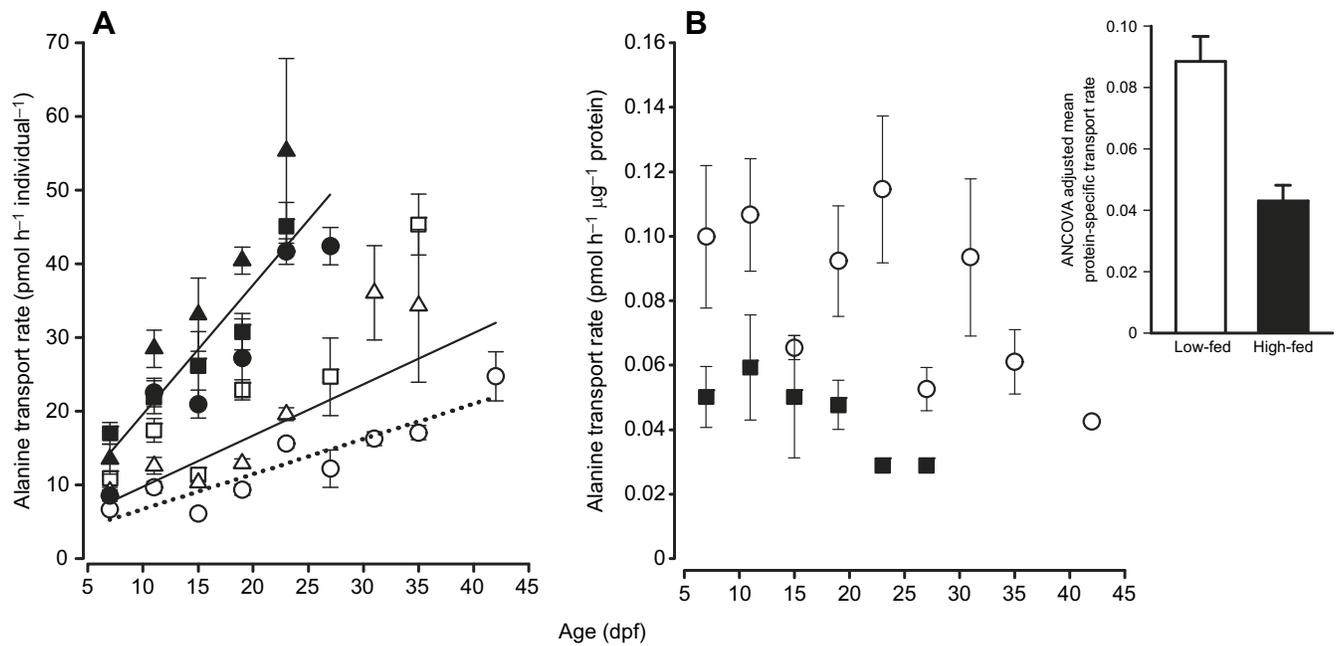
Fig. 3. Alanine transport rate in low- and high-fed larvae of *D. excentricus*. (A) Whole-animal rate of alanine transport as a function of larval age for low-fed (white symbols) and high-fed (black symbols) larvae for all three cultures analyzed (culture 1, circles; culture 2, squares; culture 3, triangles). The regression line is for all three cultures for each treatment. The dotted line represents independent regression of transport rate and larval age for low-fed larvae from culture 1 (white circles). (B) Protein-specific alanine transport rate for low-fed (white circles) and high-fed (black squares) larvae. Data are means±s.e.m. at each larval age for the three replicate cultures shown in A. Inset shows the least squares means (ANCOVA) of protein-specific transport rate (from Fig. 3B); error bars are s.e.m.

(ANOVA, $F_{1,5}=0.82$, $P=0.62$). The mean (±s.e.m., $n=6$) cost for all treatments (Fig. 5A, inset) was 4.47±0.63 J mg^{-1} protein synthesized. The specificity of anisomycin was examined by

determining its effect on the rate of alanine transport (Fig. S4). No significant differences were observed in anisomycin-exposed and non-exposed larvae (paired *t*-test: $t_5=0.96$, $P=0.38$). The cost of
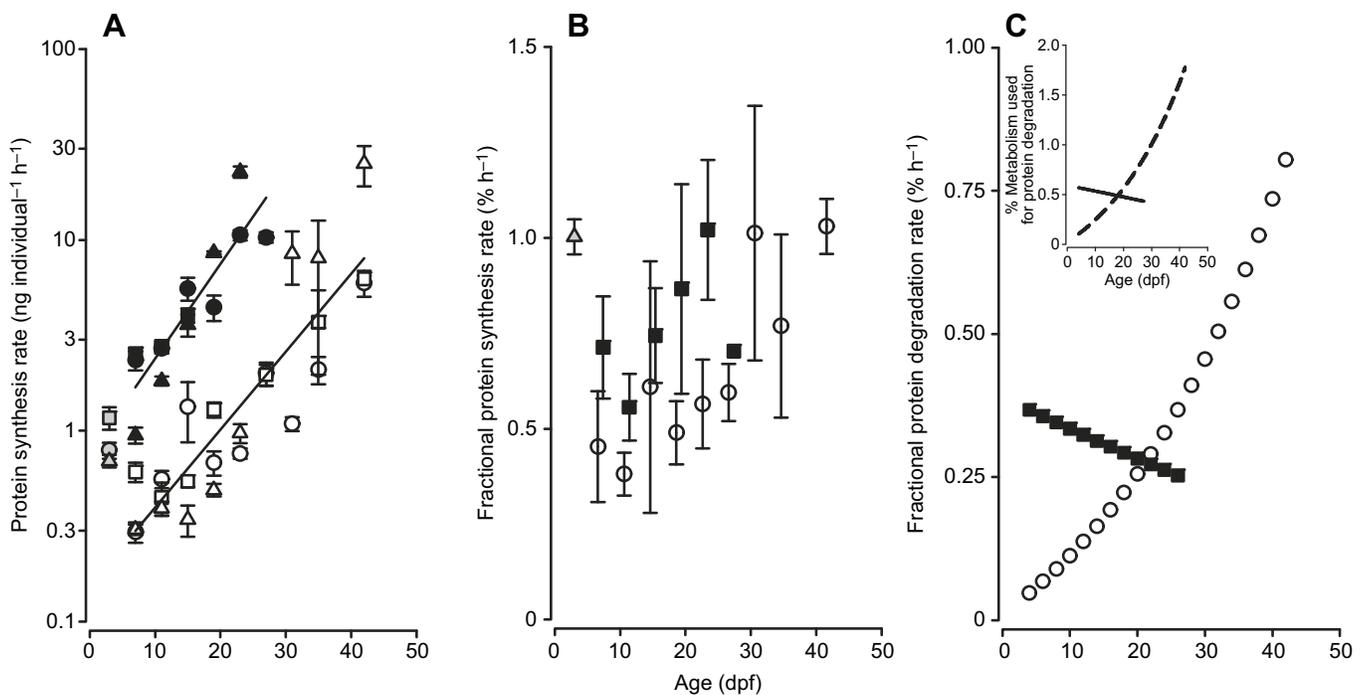
Fig. 4. Protein metabolism in low- and high-fed larvae of *D. excentricus*. (A) Whole-animal rate of protein synthesis (plotted on a log$_{10}$ scale) before feeding (gray symbols) and in low-fed (white symbols) and high-fed (black symbols) larvae as a function of age. Regression lines show the pooled response for low- and high-fed larvae for all three cultures analyzed (culture 1, circles; culture 2, squares; culture 3, triangles). (B) Fractional rate of protein synthesis before feeding (gray triangle) and in low-fed (white circles) and high-fed (black squares) larvae. Data are means±s.e.m. for the three independent cultures at each larval age, and are slightly offset for visual clarity. (C) Modeled rate of protein degradation in low-fed (white circles) and high-fed (black squares) larvae. Inset shows the estimated percentage metabolism used for protein degradation during development.
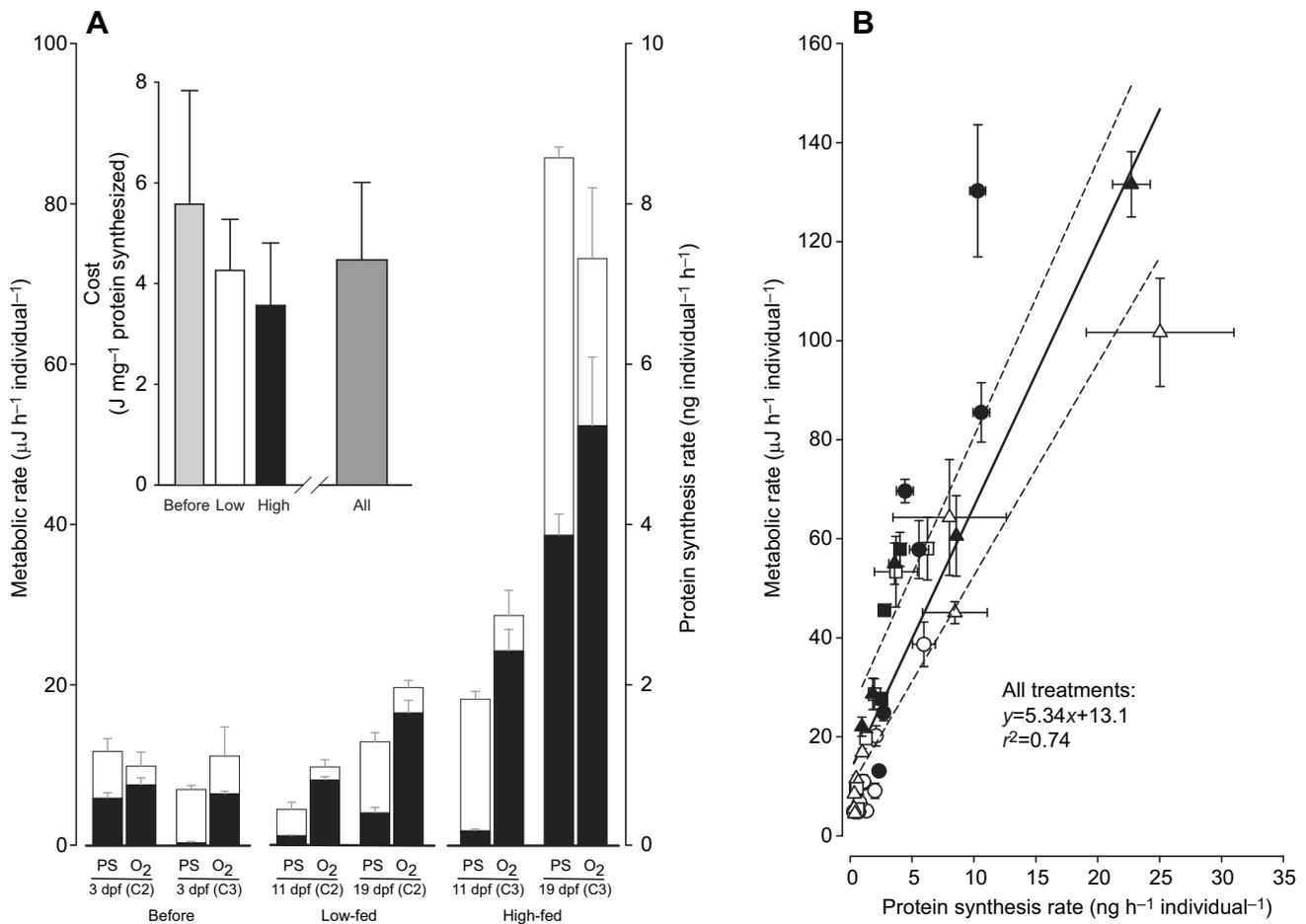
Fig. 5. Energetic cost of protein synthesis in low- and high-fed larvae of *D. excentricus*. (A) Primary data for inhibitor analysis calculating the energetic cost of protein synthesis. Rates of protein synthesis (PS, right *y*-axis) and metabolism (O_2, left *y*-axis) for the developmental stages and feeding treatments used to calculate cost (C, culture number). White bars are uninhibited rates of protein synthesis and metabolism. Black bars are respective rates in the presence of anisomycin. Inset shows the average cost before feeding, and in low-fed and high-fed larvae derived from primary data (means±s.d., *n*=2). Differences between stages/treatments were not significant (ANOVA: d.f.=1, 5, *P*=0.62) and the average cost was 4.47±0.63 J mg^{-1} protein (mean±s.e.m., *n*=6). (B) Correlative cost of protein synthesis. Metabolic rate was plotted as a function of protein synthesis rate throughout development (no inhibitor). The solid regression line represents the pooled relationship for low-fed (white) and high-fed (black) treatments (culture 1, circles; culture 2, squares; culture 3, triangles). The slope of the relationship represents the cost of protein synthesis of 5.34±0.51 J mg^{-1} protein (mean±s.e.m., *n*=33). The dashed lines above and below the solid regression line represent the correlative costs for high-fed and low-fed larvae, respectively.

protein synthesis throughout larval development (using a correlative approach) (Fig. 5B) revealed a modest difference between low- and high-fed larvae (ANOVA, $F_{1,32}$=5.29, *P*=0.028; Table 1). However, there was no significant interaction between treatment and larval age (ANOVA, $F_{1,32}$=2.16, *P*=0.152; Table 1), indicating that the slopes of the regression between metabolic rate and protein synthesis rate for low- and high-fed larvae were similar. As this energetic analysis uses only the slope of the relationship to estimate cost, a pooled regression for low- and high-fed larvae returned a cost of 5.34±0.51 J mg^{-1} protein synthesized (mean±s.e.m., *n*=33). For reference, the regressions for low- and high-fed are also shown (Fig. 5B, dashed lines), indicating similar slope values of 4.29 and 5.58 J mg^{-1} protein synthesized, respectively.

Percentage metabolism and depositional efficiency

Primary data relating to rates of protein growth (Fig. 2A), protein synthesis (Fig. 4A) and respiration (Fig. 2C) were used to model the PDE and the amount of metabolism used to support protein synthesis in low- and high-fed larvae. PDE (Fig. 6A) exhibited a trend that was similar to that observed in other physiological

efficiencies (e.g. compare with Fig. 2D). Low-fed larvae had an initial efficiency that was 1.4 times higher than that of high-fed larvae (83% and 60%, respectively). PDE decreased quickly in low-fed larvae while increasing modestly in high-fed larvae. At 24 dpf, PDE was 1.6 times higher in high-fed than in low-fed larvae (66% and 41%, respectively). When standardized to developmental stage (Fig. S3E), similar results were observed with low-fed larvae exhibiting rapidly decreasing PDE values from the 4- to 8-arm stage (from ~80% to 40% at the 4- and 8-arm stage, respectively), while high-fed PDE remained relatively similar throughout all stages at about 60%.

To further assess differences in PDE and to control for differences in rates of growth, the total amount of protein synthesized and degraded to achieve ~55 ng (early development) and ~650 ng (later development) of protein growth was determined (Fig. S5). Low-fed larvae grew 52.4 ng by 12 dpf. This growth was achieved by synthesizing 72.9 ng of protein, of which 20.5 ng was degraded, resulting in a PDE of 71.9% (i.e. 52.4/72.9=0.719). High-fed larvae grew 55.3 ng by 6 dpf with synthesis and degradation rates of 97.4 and 42.1 ng, respectively (PDE=56.8%). Protein growth of ~650 ng
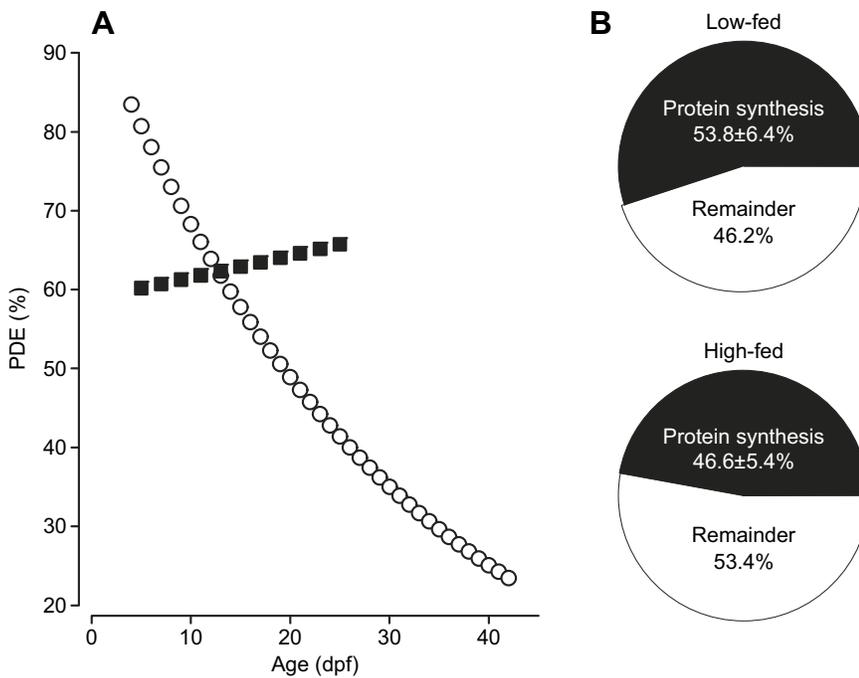
Fig. 6. Protein depositional efficiency and percentage metabolism for protein synthesis. (A) Modeled changes in protein depositional efficiency (PDE), the percentage of synthesized protein (taken from Fig. 4A) that is retained as larval biomass (taken from Fig. 2A), for low-fed (white circles) and high-fed (black squares) larvae. (B) Percentage metabolism used to fuel measured rates of protein synthesis. Protein synthesis rates (Fig. 4A) were multiplied by the grand average of the cost of protein synthesis (4.91 J mg^{-1} protein) and divided by the metabolic rate (Fig. 2C). Percentage metabolism for protein synthesis was similar between low- and high-fed larvae (ANOVA, $F_{1,32}$=0.44, P=0.51).

(Fig. S5B) occurred at 41 dpf for low-fed larvae (645.4 ng growth) and at 18 dpf for high-fed larvae (649.4 ng growth). Low-fed larvae needed to synthesize 1892 ng protein, of which 1248 ng were degraded (PDE=34.1%). High-fed larvae synthesized 1085 ng and degraded 435 ng to achieve 649.5 ng of protein growth (PDE=60.0%). Whereas high-fed larvae experienced similar increases in protein synthesis and degradation from early to late development (11.2-fold and 10.3-fold increases in synthesis and degradation, respectively), low-fed larvae exhibited a 26-fold increase in synthesis and a 62-fold increase in degradation from early to late development. These results highlight how developmental changes in degradation rates in low-fed larvae were responsible for both the high PDE in early development and the low PDE in later larval development.

To estimate the percentage metabolism used to support measured rates of protein synthesis, an average cost of protein synthesis was calculated at 4.91 J mg^{-1} protein synthesized. This cost is the average of estimates from the inhibitor and correlative approaches (4.47 and 5.34 J mg^{-1} protein synthesized, respectively). There was no significant relationship between percentage metabolic rate used for protein synthesis and larval age (ANOVA, $F_{1,32}$=0.63, P=0.432) or feeding treatment (ANOVA, $F_{1,32}$=0.44, P=0.512). The average percentage metabolism supporting protein synthesis rates for both low- and high-fed larvae was about 50% (Fig. 6B).

DISCUSSION
The goal of the current study was to define strategies relating to protein metabolism that are employed by organisms growing at different rates as a result of differing food environments. To do this, we extended our analysis of physiological plasticity in larvae of the sand dollar, *D. excentricus*. Our previous work (Rendleman et al., 2018) examining energetic growth efficiencies, using the same conditions as in this study, implicated significant differences in the synthetic efficiency and/or the energetic cost of protein metabolism. The results of the present study specifically test these ideas and show that there are both significant differences in protein metabolism and important similarities between larvae growing at different rates. These data provide empirical evidence that organisms can respond to

different food environments by exploiting different macromolecular turnover strategies to achieve growth.

Protein metabolism and differential growth during early development
The most important result of this study was that the large-scale differences in growth rate between low- and high-fed larvae were achieved by differences in mass-specific rate of protein degradation and not by differences in mass-specific rate of protein synthesis. While there were major differences in organismal rate of protein synthesis between low- and high-fed larvae, these differences were a result of high-fed larvae having a higher biomass than low-fed larvae. This is to be expected given the 10-fold difference in food availability. However, once synthesis rate was standardized to protein biomass (i.e. fractional rate of protein synthesis), rates of synthesis were similar between feeding treatments. Fractional rates of synthesis in this study of ~0.5–1% h^{-1} were similar to those for other echinoderm larvae experiencing positive growth (Pace and Manahan, 2006, 2007b; Ginsburg and Manahan, 2009).

Our analysis of PDE provides a potential explanation for the previously observed differences in organismal growth efficiencies between low- and high-fed larvae. The predominant biochemical constituent of *D. excentricus* larvae is protein (Rendleman et al., 2018). Like other efficiency metrics (AE, GGE and PGE), PDE was initially higher in low-fed larvae but quickly decreased over developmental time (from 83% to 23%). Meanwhile, PDE in high-fed larvae increased a modest amount (from 60% to 66%). Examination of these changes at specific developmental points (i.e. pluteus arm number) showed a similar trend where high-fed larvae exhibited stable PDE values while low-fed larval PDE decreased substantially. Because mass-specific rates of protein synthesis were similar in low- and high-fed larvae, the large differences in PDE were an outcome of the treatment-specific differences in mass-specific rates of protein degradation. While degradation rates of high-fed larvae decreased modestly over developmental time, those for low-fed larvae increased 17-fold. Our analysis of PDE at 55 and 650 ng of protein growth further establishes the role of protein degradation in

setting the treatment-specific differences in PDE. While rates of synthesis and degradation increased in similar proportion to each other in high-fed larvae (~10-fold), increases in low-fed larval rates of degradation substantially out-paced increases in synthesis rates (62- and 26-fold, respectively). Given the similar pattern of PDE with the other growth efficiency metrics (GGE and PGE) and the foundational requirement of macromolecular synthetic pathways for supporting growth, the differences in protein degradation rate provide at least a partial explanation for the large differences in physiological plasticity related to growth efficiencies.

No significant differences were observed in the energetic cost of protein synthesis or its metabolic regulation in low- and high-fed larvae. As protein synthesis is typically the single-most expensive metabolic process (Hawkins, 1991; Houlihan, 1991), we used two techniques to arrive at an accurate energetic estimate of this critical cost. The two estimates returned similar energetic values with an average cost of 4.91 J mg^{-1} protein synthesized. The first method relied on the eukaryotic translation inhibitor anisomycin to measure cost at specific developmental times. The second approach used a correlative method in which the average cost of synthesis over the entire range of larval development was estimated. We observed similar energetic costs of protein synthesis with respect to technique employed, developmental stage and larval feeding treatment. Our energetic determinations of cost are similar to previous studies on larval echinoderms (Pace and Manahan, 2006, 2007a; Pan et al., 2015). Using this cost of synthesis, we determined the amount of metabolic energy used to support measured rates of protein synthesis. Here too, no significant differences were observed with respect to developmental age or feeding treatment. The average percentage metabolic energy used to support measured rates of synthesis was ~50%, a value that is in agreement with other studies of marine invertebrate larvae (Pace and Manahan, 2007a; Lee et al., 2016; Pan et al., 2018).

While the rate of protein degradation was the major difference in growth efficiency between low- and high-fed larvae, the associated cost of degradation did not appear to be a significant factor in the plasticity response. The amount of metabolism required to support degradation rate increased for low-fed larvae over development; however, the estimated percentage metabolism was no more than 2%. These costs were estimated using the approach of Pan et al. (2018), relying on the cost of degradation measured by Peth et al. (2013). These estimates are for proteasomal degradation and likely have a significant amount of variance due to the folding patterns of degraded proteins, their level of ubiquitination, as well as differential costs associated with other degradation pathways. Even so, the total contribution appears to be relatively small, meaning the burden of high degradation rates is related to the high cost of resynthesizing those proteins that were degraded.

With the two treatments having similar mass-specific rate of synthesis, the same energetic cost of synthesis, and utilizing a similar proportion of metabolism to support those rates, it seems likely that there are significant differences in the types of proteins that are being made. Given the 10 times higher food availability, high-fed larvae are likely making proportionally more structural proteins that can be deposited as biomass to support larval development as well as the creation of the juvenile rudiment. With significantly less food, low-fed larvae are likely making a proportionally higher number of metabolic enzymes serving regulatory purposes (i.e. house-keeping processes). These enzymes typically experience higher rates of turnover and would be a significant contributor to the relatively higher degradation rates.

Importantly, these degradation rates increase over time and result in low-fed larvae having PDE values that are ~3 times lower than those of high-fed larvae by the end of development.

Physiological mechanisms of developmental plasticity

Previous studies have indirectly implicated the role of protein metabolism in food-induced developmental plasticity in echinoid larvae (Heyland and Hodin, 2004; Carrier et al., 2015; Rendleman et al., 2018). Heyland and Hodin (2004) demonstrated that exogenous thyroxine treatment can recapitulate the high-fed morphological phenotype (short arms, rapid rudiment development). Thyroxine is known to influence protein turnover rate (Sokoloff and Kaufman, 1961; Bates and Holder, 1988). In a transcriptomic study, Carrier et al. (2015) found evidence for the role of TOR in regulating growth and development. TOR is known to be a master regulator of protein synthesis, with high levels causing an increase in ribosome biogenesis and subsequent up-regulation of translational processes (Raught et al., 2001). The direct measurements of protein metabolism in this study support these previous studies. The action of TOR may provide an explanation for why high-fed larvae are able to maintain equivalent levels of mass-specific protein synthesis despite their very rapid increase in protein biomass. TOR is also known to negatively regulate macroautophagy. During invertebrate larval development, TOR levels decrease when there is nutritional stress, increasing rates of macroautophagy (Scott et al., 2004; Di Bartolomeo et al., 2010; Romanelli et al., 2014). This provides an explanation for the higher overall degradation rate in low-fed larvae as development proceeds, thereby allowing for the synthesis of high-turnover proteins. Adams et al. (2011) demonstrated that dopaminergic receptors respond to food environment and appear to cause the induction of the short-armed, high-fed larval phenotype. Because of the wide range of effects that dopamine can have on cellular physiology, it is difficult to know, at this time, what role it might play with regards to protein metabolism. Dopamine signaling is known to influence cellular plasticity by changing aspects of protein metabolism (Hasselgren et al., 1983; Smith et al., 2005; Pfeiffer and Huber, 2006). In *Caenorhabditis elegans*, dopamine signaling results in higher levels of proteasomal degradation by increasing polyubiquitination of protein substrates (Joshi et al., 2016). This dopaminergic response, which is located in the epithelial cells, is activated when the worm encounters a bacterial lawn for feeding. Given the highly specific location of dopamine receptors at the tips of the pluteus larva's PO arms (Adams et al., 2011), this raises the possibility that the induction of the short-armed phenotype may be driven by increased degradation rates at the larval arms. This could then allow tissue growth to be focused towards post-larval structures such as the stomach and rudiment. These results are consistent with the increases seen in PDE as high-fed larvae develop and could be the consequence of increasing levels of TOR. Future analyses testing for such morphologically specific differences in protein homeostasis, as well as examining specific pathways of protein degradation (proteasomal versus autophagy) will be important for further understanding the role of both TOR and dopamine signaling mechanisms in the plasticity response.

Our analysis of protein metabolism also indicated that amino acid transport may play a critical role in the developmental plasticity response. Low-fed larvae had rates of alanine transport that were ~2 times higher than those of high-fed larvae. This result is of interest because it is likely related to the morphological plasticity response. The long-armed phenotype of low-fed larvae has been interpreted as a means to increase their feeding ability on algal cells (Hart and Strathmann, 1994). Previous studies have demonstrated that transport of dissolved organic material (DOM) can contribute to sustaining

larval metabolism (Manahan, 1990; Shilling and Manahan, 1994) and that amino acid transporters in pluteus larvae are primarily localized to the external epithelium, including the larval arms (Meyer and Manahan, 2009). Therefore, a long-armed phenotype may also serve the purpose of allowing greater access to the DOM pool by way of increasing the epithelial surface area. Future studies specifically addressing this possibility (e.g. determining transport kinetics and maximum transport rates) will be necessary to fully evaluate this potentially adaptive response in low-fed larvae.

In total, the findings from other echinoid developmental plasticity studies in combination with the current results suggest an integrated initial response to food levels involving physiological and morphological responses which complement one another. Food conditions are sensed prior to the onset of feeding ability (Miner, 2007; Adams et al., 2011). If the larva is in a high-food environment, then dopamine signaling will cause the induction of the short-armed phenotype (Adams et al., 2011). Part of this response may involve changes in protein turnover which have a negative influence on arm length and allow greater growth in post-larval structures, resulting in initially lower PDE values in high-fed larvae (this study). If food levels are low, then the default pathway of long larval arms is followed. The longer arms allow increased feeding ability (Hart and Strathmann, 1994) and DOM transport rates (this study). Accompanying these changes are increased levels of GGE and PGE (Rendleman et al., 2018; this study). These increased growth efficiencies are supported by increased PDE (this study), which is supported by down-regulation of protein degradation (this study). It is of interest that the default, long-arm, low-fed pathway elicits greater initial protein metabolic and growth efficiency. Understanding the molecular mechanisms that allow for high efficiency growth and comparing them with larval forms that do not have developmental plasticity would be of interest.

Relating these morphological and physiological responses to their adaptive value for the entirety of larval development is critical to understanding the actual ecophysiological value of developmental plasticity. It has been observed that the differential arm length response occurs early in larval development (Boidron-Metairon, 1988; Sewell et al., 2004; Miner, 2007). Physiologically, large differences in both AE and growth efficiency (Rendleman et al., 2018; this study) that benefit low-fed larvae are also seen only in early larval development and decrease rapidly during larval development. These results may be indicative of the cost–benefit relationship between surface area exposure and nutrient acquisition. Longer arms might result in the need for greater surface area ion regulation. Ion regulation by the Na^+/K^+-ATPase pump can consume ~40% of larval metabolic energy (Leong and Manahan, 1997). Therefore, there may be a limit to the extent, both in total arm length and in developmental time, that long arms are adaptive. The long-armed phenotype may provide its greatest benefit early in the larval stage so as to allow the larva to find a more supportive nutritional environment without incurring large costs for surface area exposure. After early larval development, the survival strategy may alter to one of overall metabolic down-regulation with specific decreases in protein metabolism relating to growth in order to save energy and await better feeding conditions. In studies examining protein synthesis in unfed echinoid larvae (i.e. receiving no algal food), metabolic regulation of protein synthesis decreased to 16–21% of metabolism (Pace and Manahan, 2006; Pan et al., 2015), allowing for the maintenance of other essential processes such as Na^+/K^+-ATPase. These plastic physiological strategies likely allow for the long-term survival observed in nutritionally stressed larvae (e.g. Moran and Manahan, 2004; Carrier et al., 2015).

Echinoid larvae as a model system for developmental plasticity

The importance of developmental plasticity has been expressed by evolutionary biologists, molecular biologists, ecologists and physiologists (e.g. DeWitt et al., 1998; Miner et al., 2005; Evans and Hofmann, 2012; Uller et al., 2020). The developmental biology of sea urchins has long attracted researchers from all of these fields, resulting in a powerful set of integrative biological information. Echinoid larvae have been the subject of many studies regarding developmental plasticity (reviewed in McAlister and Miner, 2018). Importantly, these studies have shed light on the molecular, morphological and physiological manifestation of developmental plasticity. By virtue of these combined datasets, continued efforts using this system will provide a highly informative and integrated platform for understanding how organisms respond to changes in other important environmental conditions (e.g. temperature, pH, pollutants).

A critical point that has been brought up in previous analyses is the need for experimental replication. Sewell et al. (2004) observed significant within-treatment variation associated with culture chambers. Future studies should employ experimental designs by which to assess and partition this variation from the among-treatment effects (Sewell et al., 2004; McAlister and Miner, 2018). This current study, as well as our previous study on growth efficiency (Rendleman et al., 2018) employed three independent cultures (e.g. spawned at different times of the year using different parents). This was especially important given the integrative nature of our physiological measurements, which can result in relatively large amounts of variance. We did observe significant within-treatment variation for rates of ingestion, respiration and alanine transport. However, this variation did not obscure the effect of food availability. In total, we now have six independent cultures, over the course of 4 years (initiated in different seasons), that show a consensus signal in the physiological strategies that are exploited to achieve positive growth in larvae experiencing different amounts of food. It is apparent that significant physiological plasticity, specifically relating to protein synthetic efficiency, accompanies the well-characterized morphological plasticity of these larvae. Future experiments will further explore this system to discover more regarding its mechanisms and adaptive value as well as identify its linkage to other important attributes of developmental plasticity such as TOR and dopamine signaling.

Supplementary information

Supplementary information available online at
https://jeb.biologists.org/lookup/doi/10.1242/jeb.230748.supplemental

References

Adams, D. K., Sewell, M. A., Angerer, R. C. and Angerer, L. M. (2011). Rapid adaptation to food availability by a dopamine-mediated morphogenetic response. *Nat. Commun.* **2**, 592. doi:10.1038/ncomms1603

Bates, P. C. and Holder, A. T. (1988). The anabolic actions of growth hormone and thyroxine on protein metabolism in Snell dwarf and normal mice. *J. Endocrinol.* **119**, 31-41. doi:10.1677/joe.0.1190031

Berg, J. M., Tymoczko, J. L. and Stryer, L. (2012). *Biochemistry* (ed. J. M. Berg, J. L. Tymoczko, L. Stryer and Gregory J. Gatto, Jr). New York: WH Freeman.

Bertram, D. F. and Strathmann, R. R. (1998). Effects of maternal and larval nutrition on growth and form of planktotrophic larvae. *Ecology* **79**, 315-327. doi:10.1890/0012-9658(1998)079[0315:EOMALN]2.0.CO;2

Boidron-Metairon, I. F. (1988). Morphological plasticity in laboratory-reared echinoplutei of Dendraster excentricus (Eschscholtz) and Lytechinus variegatus (Lamarck) in response to food conditions. *J. Exp. Mar. Biol. Ecol.* **119**, 31-41. doi:10.1016/0022-0981(88)90150-5

Byrne, M., Sewell, M. A. and Prowse, T. A. A. (2008). Nutritional ecology of sea urchin larvae: influence of endogenous and exogenous nutrition on echinopluteal growth and phenotypic plasticity in Tripneustes gratilla. *Funct. Ecol.* **22**, 643-648. doi:10.1111/j.1365-2435.2008.01427.x

Carrier, T. J., King, B. L. and Coffman, J. A. (2015). Gene expression changes associated with the developmental plasticity of sea urchin larvae in response to food availability. *Biol. Bull.* **228**, 171-180. doi:10.1086/BBLv228n3p171

Conceição, L. E. C., Dersjant-Li, Y. and Verreth, J. A. J. (1998). Cost of growth in larval and juvenile African catfish (Clarias gariepinus) in relation to growth rate, food intake and oxygen consumption. *Aquaculture* **161**, 95-106. doi:10.1016/S0044-8486(97)00260-3

Cucci, T. L., Shumway, S. E., Brown, W. S. and Newell, C. R. (1989). Using phytoplankton and flow cytometry to analyze grazing by marine organisms. *Cytometry* **10**, 659-669. doi:10.1002/cyto.990100523

DeWitt, T. J., Sih, A. and Wilson, D. S. (1998). Costs and limits of phenotypic plasticity. *Trends Ecol. Evol.* **13**, 77-81. doi:10.1016/S0169-5347(97)01274-3

Di Bartolomeo, S., Nazio, F. and Cecconi, F. (2010). The role of autophagy during development in higher eukaryotes. *Traffic* **11**, 1280-1289. doi:10.1111/j.1600-0854.2010.01103.x

Evans, T. G. and Hofmann, G. E. (2012). Defining the limits of physiological plasticity: how gene expression can assess and predict the consequences of ocean change. *Philos. Trans. R. Soc. B Biol. Sci.* **367**, 1733-1745. doi:10.1098/rstb.2012.0019

Fenteany, G., Standaert, R., Lane, W., Choi, S., Corey, E. and Schreiber, S. (1995). Inhibition of proteasome activities and subunit-specific amino-terminal threonine modification by lactacystin. *Science* **268**, 726-731. doi:10.1126/science.7732382

Finley, D. (2009). Recognition and processing of ubiquitin-protein conjugates by the proteasome. *Annu. Rev. Biochem.* **78**, 477-513. doi:10.1146/annurev.biochem.78.081507.101607

Fraser, K. P. P. and Rogers, A. D. (2007). Protein metabolism in marine animals: the underlying mechanism of growth. *Adv. Mar. Biol.* **52**, 267-362. doi:10.1016/S0065-2881(06)52003-6

Ginsburg, D. W. and Manahan, D. T. (2009). Developmental physiology of Antarctic asteroids with different life-history modes. *Mar. Biol.* **156**, 2391-2402. doi:10.1007/s00227-009-1268-0

Gnaiger, E. (1983). Calculation of energetic and biochemical equivalents of respiratory oxygen consumption. In *Polarographic Oxygen Sensors* (ed. E. Gnaiger E. and H. Forstner), pp. 337-345. Springer. https://doi.org/10.1007/978-3-642-81863-9_30

Hart, M. W. and Strathmann, R. R. (1994). Functional consequences of phenotypic plasticity in echinoid larvae. *Biol. Bull.* **186**, 291-299. doi:10.2307/1542275

Hasselgren, P.-O., Biber, B. and Fornander, J. (1983). Improved blood flow and protein synthesis in the postischemic liver following infusion of dopamine. *J. Surg. Res.* **34**, 44-52. doi:10.1016/0022-4804(83)90020-3

Hawkins, A. J. S. (1991). Protein turnover: a functional appraisal. *Funct. Ecol.* **5**, 222-233. doi:10.2307/2389260

Heyland, A. and Hodin, J. (2004). Heterochronic developmental shift caused by thyroid hormone in larval sand dollars and its implications for phenotypic plasticity and the evolution of nonfeeding development. *Evolution* **58**, 524-538. doi:10.1111/j.0014-3820.2004.tb01676.x

Houlihan, D. F. (1991). Protein turnover in ectotherms and its relationships to energetics. *Adv. Comp. Environ. Physiol.* **7**, 1-43. doi:10.1007/978-3-642-75897-3_1

Joshi, K. K., Matlack, T. L. and Rongo, C. (2016). Dopamine signaling promotes the xenobiotic stress response and protein homeostasis. *EMBO J.* **35**, 1885-1901. doi:10.15252/embj.201592524

Lee, J. W., Applebaum, S. L. and Manahan, D. T. (2016). Metabolic cost of protein synthesis in larvae of the pacific oyster (Crassostrea gigas) is fixed across genotype, phenotype, and environmental temperature. *Biol. Bull.* **230**, 175-187. doi:10.1086/BBLv230n3p175

Leong, P. and Manahan, D. (1997). Metabolic importance of Na+/K+-ATPase activity during sea urchin development. *J. Exp. Biol.* **200**, 2881-2892.

Lindroth, P. and Mopper, K. (1979). High performance liquid chromatographic determination of subpicomole amounts of amino acids by precolumn fluorescence derivatization with o-phthaldialdehyde. *Anal. Chem.* **51**, 1667-1674. doi:10.1021/ac50047a019

Lizárraga, D., Danihel, A. and Pernet, B. (2017). Low concentrations of large inedible particles reduce feeding rates of echinoderm larvae. *Mar. Biol.* **164**, 102. doi:10.1007/s00227-017-3134-9

Manahan, D. T. (1990). Adaptations by invertebrate larvae for nutrient acquisition from seawater. *Am. Zool.* **30**, 147-160. doi:10.1093/icb/30.1.147

Marsh, A. G. and Manahan, D. T. (1999). A method for accurate measurements of the respiration rates of marine invertebrate embryos and larvae. *Mar. Ecol. Prog. Ser.* **184**, 1-10. doi:10.3354/meps184001

Marsh, A. G., Maxson, R. E. and Manahan, D. T. (2001). High macromolecular synthesis with low metabolic cost in Antarctic sea urchin embryos. *Science* **291**, 1950-1952. doi:10.1126/science.1056341

McAlister, J. S. and Miner, B. G. (2018). *Phenotypic Plasticity of Feeding Structures in Marine Invertebrate Larvae*. Oxford, UK: Oxford University Press.

McEdward, L. R. (1984). Morphometric and metabolic analysis of the growth and form of an echinopluteus. *J. Exp. Mar. Biol. Ecol.* **82**, 259-287. doi:10.1016/0022-0981(84)90109-6

Meyer, E. and Manahan, D. T. (2009). Nutrient uptake by marine invertebrates: cloning and functional analysis of amino acid transporter genes in developing sea urchins (Strongylocentrotus purpuratus). *Biol. Bull.* **217**, 6-24. doi:10.1086/BBLv217n1p6

Miner, B. G. (2007). Larval feeding structure plasticity during pre-feeding stages of echinoids: not all species respond to the same cues. *J. Exp. Mar. Biol. Ecol.* **343**, 158-165. doi:10.1016/j.jembe.2006.11.001

Miner, B. G. (2011). Mechanisms underlying feeding-structure plasticity in echinoderm larvae. In *Mechanisms of Life History Evolution: The Genetics and Physiology of Life History Traits and Trade-Offs* (ed. T. Flatt and A. Heyland), pp. 221-229. Oxford University Press. doi:10.1093/acprof:oso/9780199568765.003.0017

Miner, B. G. and Vonesh, J. R. (2004). Effects of fine grain environmental variability on morphological plasticity. *Ecol. Lett.* **7**, 794-801. doi:10.1111/j.1461-0248.2004.00637.x

Miner, B. G., Sultan, S. E., Morgan, S. G., Padilla, D. K. and Relyea, R. A. (2005). Ecological consequences of phenotypic plasticity. *Trends Ecol. Evol.* **20**, 685-692. doi:10.1016/j.tree.2005.08.002

Moran, A. L. and Manahan, D. T. (2004). Physiological recovery from prolonged 'starvation' in larvae of the Pacific oyster Crassostrea gigas. *J. Exp. Mar. Biol. Ecol.* **306**, 17-36. doi:10.1016/j.jembe.2003.12.021

Pace, D. A. and Manahan, D. T. (2006). Fixed metabolic costs for highly variable rates of protein synthesis in sea urchin embryos and larvae. *J. Exp. Biol.* **209**, 158-170. doi:10.1242/jeb.01962

Pace, D. A. and Manahan, D. T. (2007a). Cost of protein synthesis and energy allocation during development of Antarctic Sea urchin embryos and larvae. *Biol. Bull.* **212**, 115-129. doi:10.2307/25066589

Pace, D. A. and Manahan, D. T. (2007b). Efficiencies and costs of larval growth in different food environments (Asteroidea: Asterina miniata). *J. Exp. Mar. Biol. Ecol.* **353**, 89-106. doi:10.1016/j.jembe.2007.09.005

Pace, D. A., Maxson, R. and Manahan, D. T. (2010). Ribosomal analysis of rapid rates of protein synthesis in the Antarctic Sea Urchin Sterechinus neumayeri. *Biol. Bull.* **218**, 48-60. doi:10.1086/BBLv218n1p48

Pan, T.-C. F., Applebaum, S. L. and Manahan, D. T. (2015). Experimental ocean acidification alters the allocation of metabolic energy. *Proc. Natl Acad. Sci. USA* **112**, 4696-4701. doi:10.1073/pnas.1416967112

Pan, T.-C. F., Applebaum, S. L., Frieder, C. A. and Manahan, D. T. (2018). Biochemical bases of growth variation during development: a study of protein turnover in pedigreed families of bivalve larvae (Crassostrea gigas). *J. Exp. Biol.* **221**, jeb171967. doi:10.1242/jeb.171967

Peth, A., Nathan, J. A. and Goldberg, A. L. (2013). The ATP costs and time required to degrade ubiquitinated proteins by the 26 S proteasome. *J. Biol. Chem.* **288**, 29215-29222. doi:10.1074/jbc.M113.482570

Pfeiffer, B. E. and Huber, K. M. (2006). Current advances in local protein synthesis and synaptic plasticity. *J. Neurosci.* **26**, 7147-7150. doi:10.1523/JNEUROSCI.1797-06.2006

Raught, B., Gingras, A.-C. and Sonenberg, N. (2001). The target of rapamycin (TOR) proteins. *Proc. Natl Acad. Sci. USA* **98**, 7037-7044. doi:10.1073/pnas.121145898

Reitzel, A. M., Webb, J. and Arellano, S. (2004). Growth, development and condition of Dendraster excentricus (Eschscholtz) larvae reared on natural and laboratory diets. *J. Plankton Res.* **26**, 901-908. doi:10.1093/plankt/fbh077

Rendleman, A. J. and Pace, D. A. (2018). Physiology of growth in typical and transversus echinopluteus larvae. *Invertebr. Biol.* **137**, 289-307. doi:10.1111/ivb.12227

Rendleman, A. J., Rodriguez, J. A., Ohanian, A. and Pace, D. A. (2018). More than morphology: differences in food ration drive physiological plasticity in echinoid larvae. *J. Exp. Mar. Biol. Ecol.* **501**, 1-15. doi:10.1016/j.jembe.2017.12.018

Romanelli, D., Casati, B., Franzetti, E. and Tettamanti, G. (2014). A molecular view of autophagy in Lepidoptera. *BioMed Res. Int.* **2014**, 902315. doi:10.1155/2014/902315

Rumrill, S. S. (1990). Natural mortality of marine invertebrate larvae. *Ophelia* **32**, 163-198. doi:10.1080/00785236.1990.10422030

Schiopu, D., George, S. B. and Castell, J. (2006). Ingestion rates and dietary lipids affect growth and fatty acid composition of Dendraster excentricus larvae. *J. Exp. Mar. Biol. Ecol.* **328**, 47-75. doi:10.1016/j.jembe.2005.06.019

Schmidt-Nielsen, K. (1997). *Animal Physiology: Adaptation and Environment*. Cambridge University Press.

Scott, R. C., Schuldiner, O. and Neufeld, T. P. (2004). Role and regulation of starvation-induced autophagy in the Drosophila fat body. *Dev. Cell* **7**, 167-178. doi:10.1016/j.devcel.2004.07.009

Sewell, M. A., Cameron, M. J. and McArdle, B. H. (2004). Developmental plasticity in larval development in the echinometrid sea urchin Evechinus chloroticus with varying food ration. *J. Exp. Mar. Biol. Ecol.* **309**, 219-237. doi:10.1016/j.jembe.2004.03.016

Shilling, F. M. and Manahan, D. T. (1994). Energy metabolism and amino acid transport during early development of antarctic and temperate echinoderms. *Biol. Bull.* **187**, 398-407. doi:10.2307/1542296

Smith, W. B., Starck, S. R., Roberts, R. W. and Schuman, E. M. (2005). Dopaminergic stimulation of local protein synthesis enhances surface expression of GluR1 and synaptic transmission in hippocampal neurons. *Neuron* **45**, 765-779. doi:10.1016/j.neuron.2005.01.015

Soars, N. A., Prowse, T. A. A. and Byrne, M. (2009). Overview of phenotypic plasticity in echinoid larvae, Echinopluteus transversus; type vs. typical echinoplutei. *Mar. Ecol. Prog. Ser.* **383**, 113-125. doi:10.3354/meps07848

Sokal, R. R. R., James, F., Sokal, R. R. and Rohlf, F. J. (1987). *Introduction to Biostatistics*. W.H.Freeman & Co Ltd.

Sokoloff, L. and Kaufman, S. (1961). Thyroxine stimulation of amino acid incorporation into protein. *J. Biol. Chem.* **236**, 795-803. doi:10.1016/S0021-9258(18)64311-X

Strathmann, R. R. (1971). The feeding behavior of planktotrophic echinoderm larvae: mechanisms, regulation, and rates of suspensionfeeding. *J. Exp. Mar. Biol. Ecol.* **6**, 109-160. doi:10.1016/0022-0981(71)90054-2

Strathmann, R. R., Fenaux, L. and Strathmann, M. F. (1992). Heterochronic developmental plasticity in larval sea urchins and its implications for evolution of nonfeeding larvae. *Evolution* **46**, 972-986. doi:10.1111/j.1558-5646.1992.tb00613.x

Thompson, B. (2006). *Foundations of Behavioral Statistics: An Insight-Based Approach*. Guilford Press.

Uller, T., Feiner, N., Radersma, R., Jackson, I. S. C. and Rago, A. (2020). Developmental plasticity and evolutionary explanations. *Evol. Dev.* **22**, 47-55. doi:10.1111/ede.12314

Vedel, A. and Rissgård, H. (1993). Filter-feeding in the polychaete Nereis diversicolor: growth and bioenergetics. *Mar. Ecol. Prog. Ser.* **100**, 145-152. doi:10.3354/meps100145